

University of Wollongong

Research Online

Faculty of Engineering and Information
Sciences - Papers: Part B

Faculty of Engineering and Information
Sciences

2017

New and practical mathematical model of membrane fouling in an aerobic submerged membrane bioreactor

M F. R Zuthi

University of Technology Sydney, Chittagong University of Engineering and Technology

Wenshan Guo

University of Technology Sydney, wguo@uts.edu.au

Huu H. Ngo

University of Technology Sydney

Long D. Nghiem

University of Wollongong, longn@uow.edu.au

Faisal I. Hai

University of Wollongong, faisal@uow.edu.au

See next page for additional authors

Follow this and additional works at: <https://ro.uow.edu.au/eispapers1>



Part of the [Engineering Commons](#), and the [Science and Technology Studies Commons](#)

Recommended Citation

Zuthi, M F. R; Guo, Wenshan; Ngo, Huu H.; Nghiem, Long D.; Hai, Faisal I.; Xia, Siqing; Li, Jianxin; Li, Jixiang; and Liu, Yi, "New and practical mathematical model of membrane fouling in an aerobic submerged membrane bioreactor" (2017). *Faculty of Engineering and Information Sciences - Papers: Part B*. 135. <https://ro.uow.edu.au/eispapers1/135>

Research Online is the open access institutional repository for the University of Wollongong. For further information contact the UOW Library: research-pubs@uow.edu.au

New and practical mathematical model of membrane fouling in an aerobic submerged membrane bioreactor

Abstract

This study aimed to develop a practical semi-empirical mathematical model of membrane fouling that accounts for cake formation on the membrane and its pore blocking as the major processes of membrane fouling. In the developed model, the concentration of mixed liquor suspended solid is used as a lumped parameter to describe the formation of cake layer including the biofilm. The new model considers the combined effect of aeration and backwash on the foulants' detachment from the membrane. New exponential coefficients are also included in the model to describe the exponential increase of transmembrane pressure that typically occurs after the initial stage of an MBR operation. The model was validated using experimental data obtained from a lab-scale aerobic sponge-submerged membrane bioreactor (MBR), and the simulation of the model agreed well with the experimental findings.

Disciplines

Engineering | Science and Technology Studies

Publication Details

Zuthi, M., Guo, W., Ngo, H. Hao., Nghiem, D., Hai, F. I., Xia, S., Li, J., Li, J. & Liu, Y. (2017). New and practical mathematical model of membrane fouling in an aerobic submerged membrane bioreactor. *Bioresource Technology*, 238 86-94.

Authors

M F. R Zuthi, Wenshan Guo, Huu H. Ngo, Long D. Nghiem, Faisal I. Hai, Siqing Xia, Jianxin Li, Jixiang Li, and Yi Liu

1 **New and practical mathematical model of membrane fouling in an**
2 **aerobic submerged membrane bioreactor**

3 Zuthi, Mst Fazana Rahman^{a,b}, Guo, Wenshan^a, Ngo, Huu Hao.^{a*}, Nghiem, Duc Long^c,

4 Hai, Faisal. I.^c, Xia, Siqing^d, Li, Jianxin^e, Li, Jixiang^f, Liu, Yi^f

5 ^a*School of Civil and Environmental Engineering, University of Technology Sydney, Sydney,*
6 *NSW 2007, Australia*

7 ^b*Department of Civil Engineering, Chittagong University of Engineering and Technology,*
8 *Chittagong-4349, Bangladesh.*

9 ^c*School of Civil Mining and Environmental Engineering, University of Wollongong,*
10 *Wollongong, NSW 2522, Australia*

11 ^d*School of Environmental Science and Engineering Tongji University Shanghai P.R. China*

12 ^e*State Key Laboratory of Separation Membranes and Membrane Processes, School of Materials*
13 *Science and Engineering, Tianjin Polytechnic University, Tianjin 300387, China*

14 ^f*Shanghai Advanced Research Institute, Chinese Academy of Science, Zhangjiang Hi-Tech*
15 *Park, Pudong, Shanghai, China*

16
17
18
19
20
21
22
23
24
25
26
27
28
29
30
31
32
33
34
35
36
37
38
39
40 * Corresponding author: School of Civil and Environmental Engineering, University of
41 Technology, Sydney (UTS), P.O. Box 123, 15 Broadway, Ultimo, NSW 2007, Australia. Tel.:
42 +61 2 9514 2745; Fax: +61 2 9514 2633. E-mail address: h.ngo@uts.edu.au or
43 ngohuuhao121@gmail.com

45 **Abstract**

46 Membrane fouling occurs due to the dynamic development of resistances by several
47 fouling components in the membrane bioreactor (MBR). This study aims to develop a
48 practical semi-empirical mathematical model of membrane fouling that accounts for
49 cake formation on the membrane and its pore blocking as the major processes of
50 membrane fouling. In the developed model, the concentration of mixed liquor
51 suspended solid is used as a lumped parameter to describe the formation of cake layer
52 including the biofilm. The new model considers the combined effect of aeration and
53 backwash on the foulants' detachment from the membrane. New exponential
54 coefficients are also included in the model to describe the exponential increase of
55 transmembrane pressure that typically occurs after the initial stage of an MBR
56 operation. The model was validated using experimental data obtained from a lab-scale
57 aerobic sponge-submerged MBR, and the simulation of the model agrees well with the
58 experimental findings.

59

60 **Keyword:** Mathematical model, Membrane fouling, Pore blocking resistance, Cake
61 layer resistance, Membrane bioreactor.

62

63

64

65

66

67

68

69 **1. Introduction**

70 Membrane bioreactor (MBR) has been increasingly used for wastewater treatment
71 around the world because of its smaller physical footprint, lower sludge production, and
72 much higher removal efficiency compared to conventional activated sludge systems.
73 Despite its proven advantages over conventional wastewater treatment, membrane
74 fouling is still a major hindrance to the widespread commercial application of the MBR
75 technology. Fouling results in reduced productivity and frequent cleaning or
76 replacement of membrane demanding higher energy and operating cost (Kim et al.,
77 2013; Mannina and Cosenza 2013; Zhang et al., 2014). Numerous studies have so far
78 been conducted to identify/investigate the foulants (Gao et al., 2013; Lin et al., 2009;
79 Tian et al., 2011; Wang et al., 2015), the processes involved with fouling (Kim et al.,
80 2013; Qi et al., 2016; Wang et al., 2015; Zhang et al., 2016), and hence to devise
81 strategies to control fouling (Deng et al., 2015, 2016; Drews, 2010; Mannina and
82 Cosenza, 2013; Meng et al., 2009) for more efficient operation of the MBR systems.
83 However, membrane fouling is a highly complex phenomenon and an accurate
84 prediction of the fouling behaviour is still a major challenge for researchers (Cosenza et
85 al., 2013) pursuing further research in this arena.

86 Membrane fouling is the undesirable deposition and accumulation of
87 microorganisms, colloids, solutes, and cell debris within/on membranes (Meng et al.,
88 2009). The fouling process is a highly complex phenomenon as it is often
89 simultaneously caused by more than one mechanism. Nevertheless, membrane fouling
90 can broadly be categorized as internal fouling and external fouling. Suspended particles
91 of comparable sizes of the membrane pore (colloids) and of smaller sizes than the
92 membrane pore (soluble particles) cause internal fouling by pore clogging and pore

93 constriction (Busch et al., 2007). External fouling is ascribed to the cake layer formation
94 associated as well with the formation of biofilm. In most of the studies, fouling due to
95 the cake layer formation is considered as the major mechanism of fouling (Gao et al.,
96 2013; Lin et al., 2009; Meng et al., 2009; Pendashteh et al., 2011).

97 The cake layer on membrane is formed by particle; larger than the membrane pores
98 and the process is dependent on the concentration of MLSS, membrane flux and the
99 scouring energy induced by the aeration (Giraldo and LaChevallier, 2006). An optimal
100 concentration of MLSS in the bioreactor is considered as of critical concern for the
101 successful operation of an MBR system since the activated sludge with MLSS
102 concentrations exceeding 10 g/L may lead to worse filterability (Ferreira et al., 2010).
103 However, the MLSS concentration is a key but poorly understood operational parameter
104 linked to filtration resistance as far as the subdivisions of the membrane foulants are
105 concerned to identify components of cake layer, biofilm or other associated factors.
106 Apart from identifying the effects of gross MLSS concentration on fouling, researchers
107 recently have identified that the colloidal content of the mixed liquor, extra cellular
108 polymeric substances (EPS) and their fractions(carbohydrate and protein),
109 microorganisms (Gao et al., 2013) contribute more potentially to the development of
110 membrane fouling. Microorganisms have the capacity to colonize, and biofilm starts to
111 form as soon as they attach to the membrane surface and consequently contributes to the
112 formation of foulant layer (Gao et al., 2013). However, as the formation of biofilm is
113 accounted for separately in the fouling prediction, the process becomes much more
114 complex since it is composed of bound extra-polymeric substances (bEPS), group of
115 other microorganisms and water in a complex matrix.

116 Soluble microbial products (SMPs) and extra cellular polymeric substances (EPS)
117 have appeared as critical concerns when found integrated within the cake layer
118 formation. Moreover, the time-dependent characteristics of most fouling mechanisms
119 can further add to the complexity of membrane fouling in MBR applications. As a
120 consequence, mathematical model-based approach has been adopted by researchers to
121 gain further insight of the fouling phenomena especially in regards to the complex
122 interactions among the physio-biochemical conditions within MBR. A significant
123 number of modelling studies have been performed on membrane fouling employing
124 resistance-in-series model in the last decade. Most of the models are basically based on
125 cake layer formation, concentration polarization and irreversible resistance (Li and
126 Wang, 2006; Mannina et al., 2011; Wintgens et al., 2003;) . Wintgens et al. (2003)
127 presented a semi-empirical model considering the cake layer formation, concentration
128 polarization and irreversibile resistance for a submerged MBR system. Reversible and
129 irreversible cake layer, pore blocking, and the feed side hydrodynamics were covered in
130 a model by Li and Wang (2006). They used sectional approach to describe the non-
131 uniform distribution of the turbulent shear intensity and the fouling material coverage
132 on the membrane surface. Nagaoka et al. (1998) developed an approach for the biofilm
133 model of a membrane-based activated sludge system to study the influence of EPS on
134 membrane surface and the biofouling, where aeration induced shearing stress was
135 assumed as a factor for the reduction of fouling. Navaratna et al. (2012) provided
136 explanation on the biofilm production considering the production, accumulation and
137 consolidation of EPS onto the membrane surface as well as the aeration induced effects
138 of shear. With the increased concern about biofouling, Busch et al. (2007) modified the
139 model proposed by Nagaoka et al. (1998) taking into account the effect of backwashing

140 as well. They provided a set of comprehensive mathematical expressions considering
141 geometry, hydrodynamics, cake layer formation, pore blocking, polydispersed particles,
142 concentration polarization and biofilm formation. The effects of the fouling components
143 were described locally along the membrane's axis of length, with the effects of filtration
144 and backwashing considered in the expressions as well. The reduction of fouling due to
145 aeration induced shear was considered negligible in the model. Giraldo and
146 LeChevallier (2006) provided a set of differential equations to correlate the exponential
147 change of TMP with cake growth and associated headloss over time, removal of SMP
148 within cakes and in membrane pores, and the associated effects of operational factors on
149 fouling reductions.

150 However, separate descriptions of the complex effects of different fouling processes
151 and foulants' removal processes could hardly be integrated to correlate well with basic
152 external measures of fouling such as the practically observed TMP differences during
153 the operation of MBR systems. None of the above studies has taken into account the
154 combined effects of aeration and backwashing on membrane fouling. Aeration is needed
155 to provide oxygen for maintaining the vital function of activated sludge in suspension
156 and also to reduce fouling by scouring on the membrane surface (Mannina and Cosenza,
157 2013) . Although the periodic backwash cannot completely remove foulants from the
158 membrane surface, its contribution for the partial removal of foulants should be
159 addressed in the fouling model.

160 In this context, this paper describes the development of a simple mathematical model
161 of membrane fouling accounting pore blocking and cake formation as the major fouling
162 processes taking into account the effect of aeration and backwash. As the overall fouling
163 process is a dynamic one, the proposed mathematical expressions for the membrane

164 fouling processes necessarily include differential equations with time-dependent
165 variables and constants. A combined effect of aeration and backwash on the detachment
166 of foulants from the membrane, and the concept of exponential increase of TMP
167 especially after the initial stage of operation of MBR are included in the new model.
168 The model was calibrated using experimental data obtained from a lab-scale SSMBR
169 operated at a constant flux. The verification of model was done for additional data of the
170 SSMBR and the experimental results of a conventional MBR as well.

171 **2. Materials and Methods**

172 *2.1 Experimental set-up*

173 The experiment was performed on a lab-scale SSMBR system. Specifications of the
174 membrane module, sponge and operating conditions of the continuously aerated
175 SSMBR system are shown in Table 1. Both the influent and effluent flow rates were
176 controlled by a two channel pump while a separate pump was used for periodic
177 backwashing of the membrane. A pressure gauge was used to measure the
178 transmembrane pressure (TMP), and a hose air diffuser was used to provide air while an
179 airflow meter was used to maintain a constant air flow rate at 2.2 L/m² (membrane
180 surface).h. Before starting the experiment, the sponges used in the SSMBR were
181 acclimatized with the synthetic wastewater to be treated for 25 days.

182 **Table 1**

183 The sponge used in the SSMBR was reticulated porous polyester-urethane sponge
184 (PUS) and the optimum size of the sponge was used as determined previously according
185 to critical flux experiments by Guo et al. (2008). The activated sludge was taken from a
186 local wastewater treatment plant and was acclimatized with synthetic wastewater before

187 using it in the SSMBR system. The initial MLSS concentration in the bioreactor was set
188 approximately at 5g/L considering the high volumetric air flow rate used in the SSMBR
189 system. The synthetic wastewater mainly contained glucose, ammonium sulphate,
190 potassium dihydrogen orthophosphate and trace nutrients, and the composition of it was
191 the same as was used in the study by Lee et al. (2003) .NaHCO₃ or H₂SO₄ was used to
192 adjust the synthetic wastewater pH to 7.

193 *2.2 Methods of analysis*

194 The biological parameters were periodically measured during the period of the
195 SSMBR's operation. The MLSS of the sludge samples were analysed daily according to
196 standard methods (APHA, 1998) . The concentrations of SMP were analysed according
197 to modified method of Le-clech et al. (2006) and Menniti and Morgenroth (2010)
198 .After centrifugation of fresh 50 mL of mixed liquor sample was @ 3500 rpm for 30
199 mins, the supernatant was then decanted carefully and filtered using glass fiber filter
200 (Whatman 934-AH) with a nominal pore size of 1.2 µm. The filtrate was further filtered
201 using a 0.2 µm cellulose acetate filter for the analysis of SMP, and then SMP was
202 quantified as COD of the sample. COD analysis was done by COD reagent (HANNA
203 instruments) following their prescribed procedure.

204 *2.3 Measurements of resistances*

205 Before commencing the experiment, the intrinsic membrane resistance was measured in
206 distilled water at various fluxes in the range of 5 to 30 L/m².h flux at the increment of
207 5L/m².h. At the end of experiment, the membrane module was taken out of the
208 bioreactor and submerged in distilled water to measure the total resistance ($R_T = R_m +$
209 $R_p + R_c$) of the fouled membrane. R_T is the total resistance which is the combination of

210 membrane's intrinsic resistance (R_m), pore fouling resistance (R_p) and cake layer
211 resistance (R_c). Darcy's law was applied to calculate total membrane resistances (R_T)
212 following Eq. 01:

$$213 \quad J = \frac{\text{TMP}}{\mu R_T} \quad \text{Eq. 01}$$

214 where J is the permeate flux; TMP is the transmembrane pressure, μ is the viscosity of
215 the permeate at 20°C.

216 The fouled membrane was cleaned with distilled water first by gently shaking and
217 thereafter by using a soft spatula, made of sponge, to remove the deposited sludge cake
218 layer from the membrane surface, and then the resistance (R_p+R_m) was measured in
219 distilled water. Finally, the membrane was chemically cleaned with 2% citric acid for 6
220 hours to remove internal pore fouling, and then cleaned with 0.4% NaOCl and 4%
221 NaOH for 6 hours to determine the intrinsic membrane resistance (R_m) again. For the
222 calculation of daily total resistances from the measurements of TMP, the value of μ was
223 corrected for temperature as follows (Delrue et al., 2011);

$$224 \quad \mu_T = \mu_{20} e^{-.0239(T-20)} \quad \text{Eq. 02}$$

225 where T is the temperature of mixed liquor temperature in °C.

226 *2.4 Estimation of parameters of mathematical model*

227 The mathematical model equations were solved in Matlab 2014a based on the measured
228 TMP, fouling resistances, MLSS and SMP concentrations in the bioreactor of the
229 SSMBR. The algorithm used in the solution process was that of a nonlinear regression
230 analysis using *fitnlm* function. The process was run with different initial values of
231 parameters to ensure a maximum and acceptable value of R^2 (squared value of the
232 coefficient of variance).

233 **3. Model development**

234 In the simplified approach of mathematical modelling, the development of fouling of
235 the membrane is linked with biological indicator parameters such as the concentrations
236 of SMP and MLSS in the bioreactor. In this regard, the dynamic membrane fouling is
237 considered occurring in two major phases.

- 238 ▪ The internal pore fouling of the membrane is assumed to occur by the adsorption
239 of soluble particles within/onto the pores (e.g. SMP).
- 240 ▪ The external cake layer resistance to flux is assumed to occur as the main fouling
241 resistance integrated in which is the resistance due to biofilm.

242 *3.1 Resistance due to pore blocking*

243 A fraction of soluble products are adsorbed within the pores, and therefore reduces the
244 effective pore sizes as well as the surface porosity of the membrane causing the internal
245 pore fouling of the membrane. The soluble particles that are considered to cause pore
246 blocking of the membrane are the SMPs (soluble EPS of the microbial products). The
247 mathematical formulation of internal pore fouling is typically expressed by relationships
248 of pore blocking resistance with progressive reduction of the effective pore radius (r_p)
249 and effective porosity (f) of the membrane as shown by Eq. 03.

250
$$R_p = e^{(n_p t)} \frac{8h_m}{f r_p^2} \qquad \text{Eq. 03}$$

251 where h_m = membrane's effective thickness. The expression for R_p was first proposed by
252 Wiesner and Aptel (1996) and later modified by Bowen et al. (1997). An extension of
253 the mathematical expression for R_p is proposed by introducing an exponential term with
254 a factor n_p to better explain the typically observed exponential rise of TMP especially
255 after the initial stages of operation of an MBR system. The mass balance equation for

256 particles around the membrane causing the reduction of porosity is calculated following
257 Busch et al. (2007) .

$$258 \quad \rho_p \frac{df}{dt} = -4\eta_f J(t) c_{SMP}(t) \frac{m_{d,o}}{(m_{d,o})^2 - (m_{d,i})^2} \quad \text{Eq. 04}$$

259 where ρ_p is the density of biomass, c_{SMP} is the concentration of soluble particles
260 entering the pores which may be taken as c_{SMP} in the bioreactor, η_f is the average
261 fraction of soluble particles that accumulate in the pores, $m_{d,o}$ and $m_{d,i}$ are the membrane
262 outer and inner diameter respectively. Equation 04 can be rewritten as shown in Eq. 05
263 following the basic equation proposed by Giraldo and LeChevallier (2006).

$$264 \quad \frac{df}{dt} = -\alpha_f c_{SMP}(t) J(t) \quad \text{Eq. 05}$$

265 where α_f is the membrane porosity reduction coefficient to be determined from Eq. 06

$$266 \quad \alpha_f = \frac{1}{\rho_p} \cdot \frac{4\eta_f m_{d,o}}{(m_{d,o})^2 - (m_{d,i})^2} \quad \text{Eq. 06}$$

267 The differential equation to account for the effect of pore size reduction due to the
268 adsorption of soluble particles within the pores is given in Eq. 07 Giraldo and
269 LeChevallier (2006).

$$270 \quad \frac{dr_p}{dt} = -\alpha_p c_{SMP}(t) J(t) \quad \text{Eq. 07}$$

271 where, α_p = pore size reduction coefficient. The concentration of SMP in the bioreactor
272 (c_{SMP}) is a time dependent variable which depends on the design and operation of an
273 MBR system, particularly depending on the initial concentrations of MLSS.

274 *3.2 Resistance due to cake layer formation*

275 External membrane fouling is caused by the deposition of cake layer over the membrane
276 surface which gradually grows in size and thickness over time. It was found in the
277 earlier studies that the membrane fouling generally increases with the increase in the

278 MLSS concentrations (Kornboonraksa and Lee, 2009) that mainly contribute to the
279 progressive formation of cake layer on the membrane surface. The formation of the cake
280 layer on the membrane surface integrates in it the formation of biofilm. However, the
281 cake layer resistance due to the formation of biofilm is a complex process in the
282 mathematical modelling, especially due to the hardly understood process of the
283 detachment of biofilm (Busch et al., 2007) .As the formation of biofilm is inevitable in
284 an MBR system and is acknowledged as one of major causes of membrane fouling (Gao
285 et al., 2013), fouling prediction would not be complete without taking it into
286 consideration. Consequently, the formation and detachment of the biofilm layer is not
287 separately treated in the mathematical modelling, but is assumed to be integrated in the
288 process of the formation and detachment of the cake layer. The concentration of MLSS
289 in the bioreactor is taken as a gross parameter affecting the cake layer formation on the
290 membrane while the dynamic effects of the formation of biofilm and cake layer is
291 accounted for by taking the changes of MLSS concentrations in the model formulations.

292 Due to the continuous aeration and periodic backwashing in the MBR system, part of
293 the cake layer is detached from the membrane surface back into the mixed liquor
294 suspension. An average rate of detachment of the cake layer (k) is assumed to represent
295 this phenomenon which is accounted in the mass balance equation of the formation of
296 cake layer over the membrane surface. In this simplified mathematical model, the
297 variation of concentrations of MLSS (lumped parameter including SMP and bEPS and
298 other microorganisms) in the bioreactor is assumed to be linked with the net rate of the
299 attachment of cake layer (including biofilm) on the membrane surface. The cake
300 filtration effects accounting the cake compressibility is included in the mathematical
301 expressions of cake resistance (R_c) as shown in Eq. 08.

302
$$R_c = \alpha_c h_c(t) \rho_c e^{(n_c t)} \quad \text{Eq. 08}$$

303 where α_c = specific resistance of the compressible cake layer, h_c = variable depth of the
304 cake layer expressed as a first order differential function in time. Considering the mass
305 balance of the cake forming particles (e.g. MLSS) over the membrane surface, the h_c
306 can be expressed in the following differential equation:

307
$$\rho_c \frac{dh_c}{dt} = J \cdot (1 - k) c_c(t) \quad \text{Eq. 09}$$

308 where c_c = concentration of potential cake forming particles in the bulk liquid (e.g.
309 MLSS) which typically varies over time, ρ_c = density of the cake layer .The factor k
310 accounts for the detachment of the cake layer from the membrane surface a reasonable
311 value for which may be determined from the model calibration. The depth of the cake
312 layer (h_c) is calculated from the solution of Eq. 09 and is replaced in Eq. 08 to calculate
313 the value of R_c . Finally, the total resistance is calculated from the equation of the
314 resistance-in-series model as follows:

315
$$R_T = R_m + R_p + R_c \quad \text{Eq. 10}$$

316 Here the intrinsic membrane resistance (R_m) is a static component in the mathematical
317 expression which can be determined experimentally, but the total membrane resistance
318 (R_T) becomes a dynamic variable as it includes R_p and R_c . The external physical
319 parameter indicative of the membrane fouling at any stage of the operation of an MBR
320 system is the TMP (or ΔP). The state of fouling of the membrane at any instance of time
321 (t) can be obtained from the current TMP(t) the mathematical expression for which are
322 related to the respective measured data of flux (J) and total internal resistance (R_t) to
323 flux according to Darcy's law as shown in Eq. 01.

324

325 **4. Results and Discussion**

326 *4.1 Variation of MLSS and SMP with operation time*

327 The operation of full-scale MBR systems are typically done with MLSS concentrations
328 in the range of 8 to 18 g/L (Drews 2010). Among the two common practices in the
329 operation of the MBR systems, one is to keep the MLSS concentration fixed more or
330 less around a certain value which, however, needs frequent removal of excess sludge or
331 activated sludge from the mixed liquor to avoid any instability in the operation of
332 treatment such as to avoid the rapid rise of TMP. In the continuously operated MBR
333 systems without sludge removal, the concentration of MLSS often increases steadily in
334 most of the MBR systems depending on the feed characteristics and microbes present in
335 the sludge (Hernandez et al., 2015). From the operational point of view, the latter
336 practice of the MBR operation may offer advantages, for example it may promote more
337 nitrification process due to the development of nitrifying bacterial community in the
338 increased MLSS concentration (Kornboonraksha and Lee, 2009). Nevertheless, the
339 excess activated sludge may need to be withdrawn in the continuously operated MBR
340 systems to maintain its operation for longer term or to avoid any sudden instability in its
341 operation. In a study of an MBR system for treating domestic wastewater, Hasar et al. (
342 2002) had to withdraw sludge in two stages to sustain stability in the operation of the
343 systems as the MLSS steadily increased to much higher value resulting in rapid rise of
344 TMP.

345 In this study, the SSMBR system was operated upto 49 days starting with the
346 initial MLSS concentration of 5 g/L. The MLSS concentration steadily increased to 18.8
347 g/L upto 32 days of operation of the system when the rapid rise of TMP was first
348 observed. Consequently, some sludge was withdrawn (to reduce the MLSS

349 concentration around 10 g/L) after 32 days to avoid the rapid rise in TMP. The MLSS
350 again steadily increased from 10 g/L to 17 g/L up to 49 days when the operation of the
351 system was terminated since the TMP increased to about 50 kPa.

352 The effects of the withdrawal of sludge at 32 days were also evident in the
353 concentrations SMP in the bioreactor of the SSMBR. The concentration of SMP in the
354 bioreactor of MBR depends on the microbial activity, membrane rejection efficiency
355 and many other factors. During the first 32 days of operation of the SSMBR, the SMP
356 concentration was found in the range of 15 to 39 mg COD/L but relatively lower SMP
357 concentrations (15 to 22 mg COD/L) were found in the latter stage of the operation
358 period. Menniti and Morgenroth (2010) studied an MBR system under different
359 operating conditions created by high shear and low shear aerations and with different
360 membrane size. In the high shear MBR, the SMP concentration in the bioreactor was
361 found to be around 50 to 100 mg COD/L, while the SMP concentration in the low shear
362 MBR varied within the range between 50 and 350 mg COD/L.

363 *4.2 Model analysis and application*

364 *4.2.1 Inputs for model calibration*

365 In the calibration of the model, the MLSS and SMP concentrations in the bioreactor are
366 input, and these are the best representative mathematical functions of time obtained
367 from experimental data for the solution of Eq. 07 and Eq. 09. The data chosen to derive
368 the functions are the representative data measured during the first 30 days of the
369 operation of the SSMBR system. The variation of the concentrations of MLSS (in g/L)
370 up to 32 days of operation of the system can be best represented by a linear function

371 with a reasonably good correlation coefficient ($R^2= 0.95$), as shown in Eq. 11 and in
372 Figure 1.

$$373 \quad \text{MLSS} = 0.41 t + 5.6 \quad \text{Eq. 11}$$

374 Where t represents the days of operation of the SSMBR. In any continuously operated
375 MBR systems with no sludge withdrawal, the MLSS concentrations mostly increase at a
376 steady rate (Harnandez et al., 2009; Kornboonraksha and Lee, 2012). Therefore, this
377 type of best approximated function may be developed for the typical MBR system's
378 operation.

379 **Figure 1**

380 The variations of the concentrations of SMP in the bioreactor for the first 32 days of
381 operation of the MBR can be better represented by power function ($R^2: 0.79$), as shown
382 in Eq. 12 and in Figure 1.

$$383 \quad c_{\text{SMP}} = 16.3*(t)^{0.24} \quad \text{Eq. 12}$$

384 The numerical model simulation would be more simple if the rate of change of
385 MLSS or SMP concentration is given as best approximated functions. The best
386 approximated functions, as that are found in this study, may not be found in other MBR
387 systems although with continuous operations of the system. In fact, the dynamic change
388 of SMP concentration within bioreactor depends on the SMP growth rate, rate of
389 degradation, the membrane rejection efficiency and many other factors. Menniti and
390 Morgenroth (2010) found fluctuating (no trend) concentration of SMP in a high shear
391 MBR while the SMP concentration steadily increased in a low shear MBR. However,
392 the proposed model's simulation can also be done by the inputs of discrete value of
393 these parameters.

394 With specific operational and design parameters as indicated in Table 1, the value of
395 the membrane porosity reduction coefficient (α_f) was determined to be $3.25 \text{ m}^2/\text{Kg}$
396 according to Eq. 06 while the value for the membrane pore size reduction coefficient
397 (α_p) is reasonably assumed to be $0.000943 \text{ m}^3/\text{Kg}$ ($=1/\rho_p$). An average value for the
398 specific cake resistance $\alpha_c = 1 * 10^{14} \text{ m/Kg}$ was adopted which fell between the upper
399 and lower bound value as reported in the literature (Li and Wang, 2006). With other
400 design and operational parameters (e.g. measured values of J , μ , R_m) of the SSMBR and
401 the expressions for R_p and R_c are derived from Eq. 03 and Eq. 08 respectively, TMP was
402 calculated according to Darcy's law (as shown in Eq. 01).

403 *4.2.2 Model calibration and reliability analysis*

404 The unknowns involved in the solution of the mathematical expressions have some
405 characteristic features by definition. The coefficients n_p and n_c should preferably have
406 positive values, the value of effective initial porosity of the membrane should be in the
407 range between 5% and 34% (Yoon et al., 2006), and the coefficient for the rate of cake
408 layer detachment (k) should have a value between 0 and 1. With the input values of
409 variable TMP (experimental) for the first 32 days of operation of the MBR, the resulting
410 equation for TMP (according to Eq. 01) could be solved by non-linear regression
411 analysis to find unknowns and hence to simulate a reasonable TMP (Figure 2).

412 **Figure 2**

413 However, the unknown parameters and constants determined from the combined
414 mathematical modelling of total resistances $R_T (=R_m+R_p+R_c)$ against experimental TMP
415 are meaningless according to their definition in the model equations (e.g. $k \gg 1$).
416 Although the total resistance (R_T) could be predicted fairly accurately, the boundary
417 values of R_p and R_c as determined from these coefficients do not satisfy the values that

418 were experimentally measured at the end of operation of the SSMBR. Therefore, the
419 calibration of the mathematical model of membrane fouling was done separately for the
420 two dynamic components of fouling resistances, R_p and R_c . The initial and final
421 boundary values of R_p that are used for the model calibration are zero and $3.5 \cdot 10^{12}$ /m,
422 respectively. Figure 3 shows simulated results of R_p with different assumed values of
423 effective initial porosity as 7%, 10%, 15% and 25% of the membrane.

424 **Figure 3**

425 The values of the coefficients and constants as determined from the model
426 simulations for R_p are then used for further simulations for TMP against R_T to determine
427 other coefficients and constants. Table 2 shows the calculated values of all the model
428 parameters obtained from the mathematical model simulations using the data for the
429 first 32 days of operation of the SSMBR system. However, the respective values of cake
430 layer resistance (R_c) and the pore fouling resistance (R_p) at the end of day 49 of the
431 SSMBR's operation are also included in Table 2. Table 2 shows that the calculated
432 values of coefficients are meaningful and reasonable when the initial porosities of
433 membrane are below 15%. The calculated rate of cake layer detachment (the value of the
434 coefficient, k), for example, should be a positive number with a value less than 1 which
435 could only be found when the initial porosities of the membrane was assumed to be
436 between 7% and 15%. At the same time, the assumed porosity between 7% and 15% is
437 also a reasonable assumption for the microfiltration membrane. The cake layer
438 resistance R_c , as determined by the model simulation with assumed effective initial
439 porosity of 15%, is found to $1.205 \cdot 10^{13}$ /m. The measured cake layer resistance
440 ($1.07 \cdot 10^{13}$ /m) at day 49, however, was less than that determined from the model
441 simulations. This is reasonable as a fraction of the sludge was withdrawn at day 32 of

442 the SSMBR's operation. An even better agreement with the experimentally measured
443 pore fouling resistance (R_p) at day 49 could be found by the model simulation results as
444 shown in Table 2. Therefore, an effective initial porosity of 15% seems to be reasonable
445 for the membrane of the SSMBR considering the better agreement for both the
446 boundary values of R_p and R_c .

447 **Table 2**

448 **Table 3**

449 *4.2.3 Comparison between experimental and simulated results*

450 The model of membrane fouling described in this paper has introduced two new
451 parameters n_p and n_c , respectively to account for the exponential rise of dynamic
452 resistances R_p and R_c that are typically comparable with the exponential rise of TMP
453 especially after the initial stage of operation of any MBR. The model could not be
454 calibrated against the boundary values of R_p and R_c without using these exponential
455 parameters. Figure 4, for example, shows the model simulation results for R_p with and
456 without using the parameter n_p in the expression for R_p . It is evident from the simulation
457 results that the rise of pore fouling resistance without exponential parameter in the
458 model is very insignificant which does not fit the typical observations of the increase of
459 R_p in any MBR system which is also comparable to the pattern of TMP rise.

460 **Figure 4**

461 Meaningful values of the model parameters and coefficients can only be calculated
462 by the calibration of the model separately for the two dynamic components of fouling
463 resistances, R_p and R_c . The boundary values of R_p and R_c as determined by the calibrated

464 model agree reasonably well with their experimentally determined values although only
465 few selected experimental measures of TMP have been used for the calibration of the
466 model. Figure 5 shows that the experimental R_p+R_c also compares well against the daily
467 variations of simulated R_p+R_c particularly for the period when exponential increase of
468 fouling resistances/ TMP occurred. Figure 5 also shows experimental results of total
469 fouling resistance (R_T) against the daily variations of simulated R_T in terms of TMP.
470 Therefore, the mathematical model can be effectively used to predict separate
471 components of the dynamic fouling resistances along with the prediction of total fouling
472 resistances.

473 **Figure 5**

474 The model simulation was also carried out to compare the rise of TMP in a
475 conventional MBR system (CMBR, without sponges in the bioreactor) of the same type
476 that was run with a reduced constant flux ($10 \text{ L/m}^2/\text{hr}$) but with nearly the same initial
477 MLSS concentrations of the sludge (5.7 g/L) as that of the SSMBR. The wastewater
478 characteristics and the volume of the reactors are same in both the MBR systems. The
479 mean pore size of the membrane of the CMBR is $0.2 \mu\text{m}$. The model simulation has
480 been done by using the calibrated model parameters and coefficients of the SSMBR, but
481 changing the parameters relevant to the operational parameters of the CMBR (e.g. J).
482 Figure 6 shows the model simulation results of TMP of the CMBR as compared to the
483 experimentally measured results.

484 **Figure 6**

485 As was experimentally observed for the CMBR, the exponential rise of TMP cannot
486 be simulated well (Figure 6) without changing the exponential parameter (n_c) for the
487 cake layer resistance (R_c). The fundamental difference between the operation of CMBR

488 and SSMBR system is that the sponges in the bioreactor of a SSMBR act against the
489 cake layer growth and hence reduce the exponential rise of TMP due to the formation of
490 the cake layer. The fact is also evident in the model simulation results of the CMBR
491 where the cake layer resistance (R_c) cannot be simulated accurately with the same value
492 of the coefficient n_c as used for the SSMBR ($n_c=0.065$). However, the cake layer
493 resistance (R_c) and hence the TMP in the CMBR can be simulated reasonably well by
494 simply changing the value of n_c to 0.140 which accounts for more rapid rise of TMP in
495 the CMBR. Figure 6 shows the model simulation results of TMP of the CMBR with the
496 modified value of $n_c= 0.140$ instead of 0.065.

497 **5. Conclusion**

498 A new and practical semi-empirical mathematical model of membrane fouling has been
499 developed in the study that accounts pore blocking and cake formation on membrane as
500 the major processes of membrane fouling in an aerobic submerged MBR. SMPs are
501 considered as the key components of pore fouling while MLSS are assumed as
502 contributors of foulants of cake layer including the biofilm. The model simulation could
503 predict reasonably well the development fouling in a lab-scale submerged MBR system.
504 However further verification of the model is required by operating the MBR systems
505 with different MLSS concentrations and at different operating conditions.

506 **Acknowledgments**

507 This study was supported by Sustainable Water Group, MBR project, Wastewater
508 Treatment and Reuse Technologies, Centre for Technology in Water and Wastewater
509 (CTWW), School of Civil and Environmental Engineering, University of Technology,

510 Sydney (UTS). The authors are also grateful for the research collaboration of the joint
511 MBR Centre founded by UTS, Tongji University and Tianjin Polytechnic University.

512 **References:**

- 513 1. APHA., AWWA., WEF., 1998. Standard Methods for the examination of Water
514 and Wastewater. 20th edition, American Public Health Association.
- 515 2. Bowen, W. R., Mohammad, A. W., Hilai, N., 1997. Characterisation of
516 nanofiltration membranes for predictive purposes - use of salts, uncharged
517 solutes and atomic force microscopy. *Journal of Membrane Science* 126, 91-
518 105.
- 519 3. Busch, J., Cruse, A., Marquardt, W., 2007. Modeling submerged hollow-fiber
520 membrane filtration for wastewater treatment. *Journal of Membrane Science*
521 288, 94–111.
- 522 4. Cosenza, A., di Bella, G., Mannina, G., Torregrossa, M., 2013. The role of EPS
523 in fouling and foaming phenomena for a membrane bioreactor. *Bioresource*
524 *Technology* 147, 184-192.
- 525 5. Delrue, F., Stricker, A.E, Mietton-Peuchot, M., Racault, Y., 2011. Relationships
526 between mixed liquor properties, operating conditions and fouling on two full-
527 scale MBR plants. *Desalination* 272, 9–19.
- 528 6. Deng, L., Guo, W., Ngo, H. H., Zuthi, M. F. R., Zhang, J., Liang, S.,
529 Li, J., Wang, J., Zhang, X., 2015. Membrane fouling reduction and
530 improvement of sludge characteristics by bioflocculant addition in submerged
531 membrane bioreactor. 156, 450-458.
- 532 7. Deng, L., Guo, W., Ngo, H. H., Du, B., Wei, Q., Tran, N. H., Nguyen, N. C.,
533 Chen, S., Li, J. 2016. Effects of hydraulic retention time and bioflocculant

- 534 addition on membrane fouling in a sponge-submerged membrane bioreactor.
535 *Bioresource Technology*, 210, 11–17
- 536 8. Drews, A., 2010. Membrane fouling in membrane bioreactors - characterization,
537 contradiction, causes and cures. *Journal of Membrane Science* 363, 1-28.
- 538 9. Ferreira, M. L., Geilvoet, S., Moreau, A., Atasoy, E., Krzeminski, P., van
539 Nieuwenhuijzen, A., J. van der Graaf, J., 2010. MLSS concentration: Still a
540 poorly understood parameter in MBR filterability. *Desalination* 250, 618–622.
- 541 10. Gao, W.J., Han, M.N., Qu, X., Xu, C., Liao, B.Q., 2013. Characteristics of
542 wastewater and mixed liquor and their role in membrane fouling. *Bioresource*
543 *Technology* 128, 207–214.
- 544 11. Giraldo, E., LeChevallier, M., 2006. Dynamic mathematical modeling of
545 membrane fouling in submerged membrane bioreactors. *Water Environment*
546 *Foundation WEFTEC®.06*, 4895-4913.
- 547 12. Guo, W. S., Ngo, H. H., Vigneswaran, S., Xing, W., Goteti, P., 2008. A novel
548 sponge-submerged membrane bioreactor (SSMBR) for wastewater treatment
549 and reuse. *Separation Science and Technology* 43, 273–285.
- 550 13. Hasar, H, Kmacl, C., Unlii, A., 2002. Viability of microbial mass in a
551 submerged membrane bioreactor. *Desalination* 150, 263-268.
- 552 14. Hernández, L. R., García, A., L., E., Tejero, I., 2014. Comparison between a
553 fixed bed hybrid membrane bioreactor and a conventional membrane bioreactor
554 for municipal wastewater treatment: A pilot-scale study. *Bioresource*
555 *Technology* 152, 212–219.
- 556 15. Kim, M., Sankararao, B, Lee, S., Yoo, C, 2013. Prediction and identification of
557 membrane fouling mechanism in a membrane bioreactor using a combined

558 mechanistic model. *Industrial and Engineering Chemistry Research*, American
559 Chemical Society 52, 17198-17205.

560 16. Kornboonraksa, T., Lee, S. H., 2009. Factors affecting the performance of
561 membrane bioreactor for piggery wastewater treatment. *Bioresource Technology*
562 100, 2926–2932.

563 17. Le-Clech, P., Chen, V., Fane, T.A.G., 2006. Fouling in membrane bioreactors
564 used in wastewater treatment. *Journal of Membrane Science* 284 (1–2), 17-53.

565 18. Lee, W., Kang S., Shin, H., 2003. Sludge characteristics and their contribution to
566 microfiltration in submerged membrane bioreactors. *Journal of Membrane*
567 *Science* 216, 217–227.

568 19. Li, X.Y., Wang, X.M., 2006. Modelling of membrane fouling in a submerged
569 membrane bioreactor. *Journal of Membrane Science* 278, 151–161.

570 20. Lin, H. J., Xie, K., Mahendran, B., Bagley D. M., Leung, K. T., Liss, S. N.,
571 Liao, B. Q., 2009. Sludge properties and their effects on membrane fouling in
572 submerged anaerobic bioreactors (SAnMBRs). *Water Research* 43, 3827- 3837.

573 21. Mannina, G., Cosenza, A., 2013. The fouling phenomenon in membrane
574 bioreactors: Assessment of different strategies for energy saving. *Journal of*
575 *Membrane Science* 4443, 32–344.

576 22. Mannina, G., di Bella, G., Viviani, G., 2011. An integrated model for biological
577 and physical process simulation in membrane bioreactors, *Journal of Membrane*
578 *Science* 376, 56-69.

579 23. Meng, F., Chae, S., Drews, A. Kraume, M., Shin, H., Yang, F., 2009. Recent
580 advances in membrane bioreactors (MBRs): Membrane fouling and membrane
581 material. *Water Research* 43, 1489-1512.

- 582 24. Menniti, A., Morgenroth, E., 2010. Mechanisms of SMP production in
583 membrane bioreactors: Choosing an appropriate mathematical model structure.
584 Water Research 44, 5240–5251.
- 585 25. Nagaoka, H., Yamanishi, S., Miya, A., 1998. Modeling of biofouling by
586 extracellular polymers in a membrane separation activated sludge system. Water
587 Science and Technology 38 (4/5), 497–504.
- 588 26. Navaratna, D., Shu, L., Baskaran, K., Jegatheesan, V., 2012. Model
589 development and parameter estimation for a hybrid submerged membrane
590 bioreactor treating Ametryn. Bioresource Technology 113, 191–200.
- 591 27. Pendashteh, R., Fakhru'l-Razi, A., Madaeni, S. S., Abdullah, L. C., Abidin, Z.
592 Z., Biak, D. R. A., 2011. Membrane foulants characterization in a membrane
593 bioreactor (MBR) treating hypersaline oily wastewater. Chemical Engineering
594 Journal 68, 140–150.
- 595 28. Qi, C., Wang, J., Lin, Y., 2016. New insight into influence of mechanical
596 stirring on membrane fouling of membrane bioreactor: Mixed liquor properties
597 and hydrodynamic conditions. Bioresource Technology 211, 654–663
- 598 29. Tian, Y., Chen, L., Zhang, S., Zhang, S., 2011. A systematic study of soluble
599 microbial products and their fouling impacts in membrane bioreactors. Chemical
600 Engineering Journal 168, 1093–1102.
- 601 30. Wang, C., Chen, W., Hu, Q., Ji, M., Gao, X., 2015. Dynamic fouling behavior
602 and cake layer structure changes in nonwoven membrane bioreactor for bath
603 wastewater treatment, Chemical Engineering Journal 264, 462–469.

- 604 31. Wiesner, M.R., Aptel, P., 1996. Mass Transport and Permeate Flux and Fouling
605 in Pressure-Driven Processes. Water Treatment. Membrane Process, AWWA-
606 McGrawHill.
- 607 32. Wintgens, T., Rosen, J., Melin, T., Brepols, C., Drensla, K., Engelhardt, N.,
608 2003. Modelling of a membrane bioreactor system for municipal wastewater
609 treatment. Journal of Membrane Science 216 (1-2), 55-65.
- 610 33. Yoon, K., Kim, K., Wang, X., Fang, D., Hsiao, B. S., Chu, B., 2006. High flux
611 ultrafiltration membranes based on electrospun nanofibrous PAN scaffolds and
612 chitosan coating. Polymer 47, 2434-2441.
- 613 34. Zhang, M., Peng, W., Chen, J., He, Y., Ding, L., Wang, A., Lin, H., Hong, H.,
614 Zhang, Y., Yu, H., 2013. A new insight into membrane fouling mechanism in
615 submerged membrane bioreactor: Osmotic pressure during cake layer filtration.
616 Water Research 47, 2777-2786.
- 617 35. Zhang, Y., Zhang, M., Wang, F., Hong, H., Wang, A., Wang, J., Weng, X., Lin,
618 H., 2014. Membrane fouling in a submerged membrane bioreactor: Effect of pH
619 and its implications. Bioresource Technology 152, 7-14.
620

Highlights

- Fouling in MBR occurs due to dynamic development of several fouling resistances
- Pore blocking and cake layer formation on membrane are the major processes of fouling
- SMP is assumed to be the major contributor of membrane pore fouling
- MLSS is assumed to contribute to the development of cake layer and biofilm formation
- New simplified model of membrane fouling can simulate well the exponential TMP rise

Table Titles

Table 1: Design parameters, operating conditions and system performance of the SSMBR

Table 2: Parameters and model simulation results with various porosities of membrane

Table 3: Calibrated model parameters and coefficients used in simulations

Table 1

<u>Membrane details:</u>	
Membrane material	Polyethylene with hydrophilic coating
Manufacturer	Mitsubishi-Rayon, Tokyo, Japan
Pore size	0.1 μm
Outer diameter, $m_{d,o}$	0.41 mm
Inner diameter, $m_{d,i}$	0.27 mm
Effective thickness, $h_m = m_{d,o} - m_{d,i}$	0.14 mm
Surface area	0.195 m^2
<u>Sponge details:</u>	
Manufacturer's Name	Joyce Foam Products, Australia
Material	Reticulated porous polyester-urethane (PUS)
Density	28-30 kg/m^3 with 90 cells per 25 mm
Size	1 cm \times 1 cm \times 1 cm
Volume fraction of bioreactor	10%
<u>Operating conditions:</u>	
Flux, J ($\text{L}/\text{m}^2 \cdot \text{h}$)	12
Reactor volume (L)	10
MLSS (g/L)	5-18
Temperature ($^{\circ}\text{C}$)	21-24.5
Aeration rate ($\text{L}/\text{m}^2 \cdot \text{h}$)	2.2
HRT (h)	4.3
DO (mg/L)	7.5-8.5
Operation period (d)	50
Physical cleaning frequency(Backwash)	1 min after every 1 hour of filtration
Backwash rate ($\text{L}/\text{m}^2 \cdot \text{h}$)	30
<u>Influent characteristics:</u>	
COD (mg/L)	350-380
$\text{PO}_4\text{-P}$ (mg/L)	3.1-4.0
$\text{NH}_4\text{-N}$ (mg/L)	9-15
Organic Loading Rate (g COD/L/d)	1.96 - 2.1
<u>Removal efficiency (%):</u>	
COD	95-98
$\text{PO}_4\text{-P}$	85-100
$\text{NH}_4\text{-N}$	70-90

Table 2

Parameters	Initial porosities (%)			
	7	10	15	18
K	0.07	0.067	0.025	-0.007
n_p	0.081	0.089	0.097	0.107
n_c	0.231	0.118	0.065	0.065
$R_c(/m)$	$1.230 \cdot 10^{13}$	$1.204 \cdot 10^{13}$	$1.205 \cdot 10^{13}$	$9.830 \cdot 10^{14}$
$R_p(/m)$	$3.5 \cdot 10^{12}$	$3.5 \cdot 10^{12}$	$3.5 \cdot 10^{12}$	$3.5 \cdot 10^{12}$

Table 3

Parameter	Description	Value
K	rate of detachment of cake layer due to the combined effects of backwash and aeration (%)	0.025
α_c	specific cake resistance (m/Kg)	1×10^{14}
α_f	membrane porosity reduction coefficient (m ² /Kg)	3.25
α_p	pore size reduction coefficient (m ³ /Kg)	0.000943
n_c	exponential parameter (used in cake layer resistance)	0.065
n_p	exponential parameter (used in pore resistance)	0.097
R_m	membrane's intrinsic resistance (/m)	7.43×10^{11}

Figure Captions

Figure 1: Variation of MLSS and SMP in bioreactor during first 32 days of the SSMBR operation

Figure 2: Comparison of the experimentally measured TMP and the TMP calculated from mathematical model (for the first 32 days of operation of the SSMBR)

Figure 3: Simulated R_p for various initial porosities of membrane

Figure 4: Simulated R_p with and without using the parameter n_p (for porosity of 15%)

Figure 5: Comparison of model simulation results with experimental results of SSMBR (R_p+R_c and TMP)

Figure 6: Comparison of simulated TMP with experimental TMP of the CMBR (with and without modified value of exponent coefficient n_c of the model)

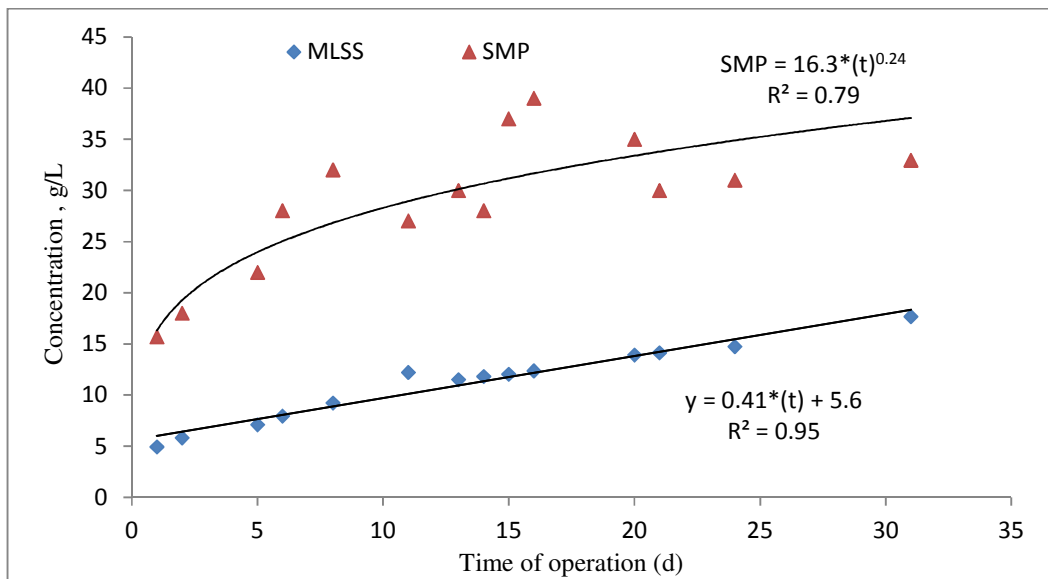


Figure 1

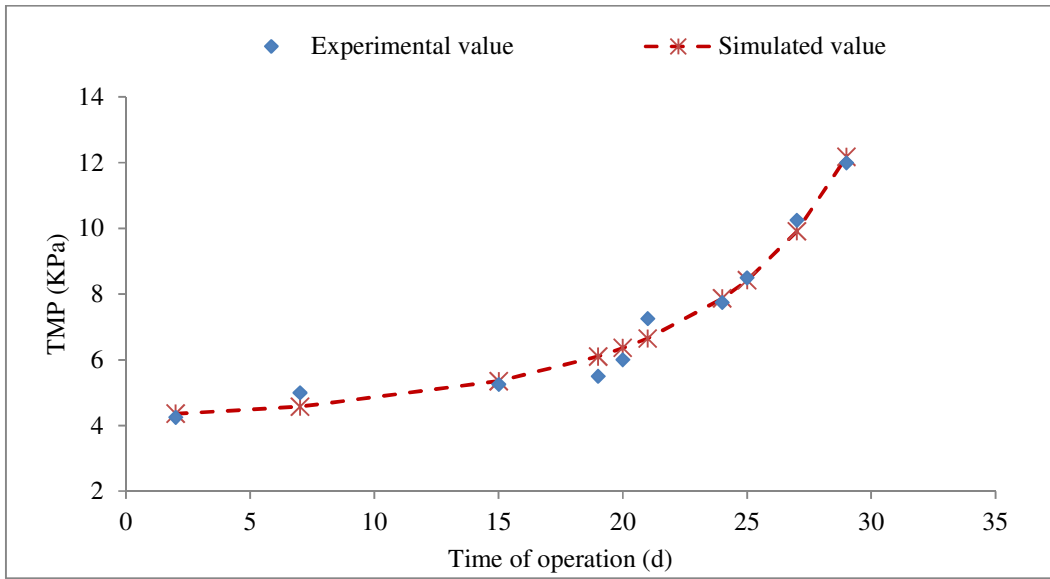


Figure 2

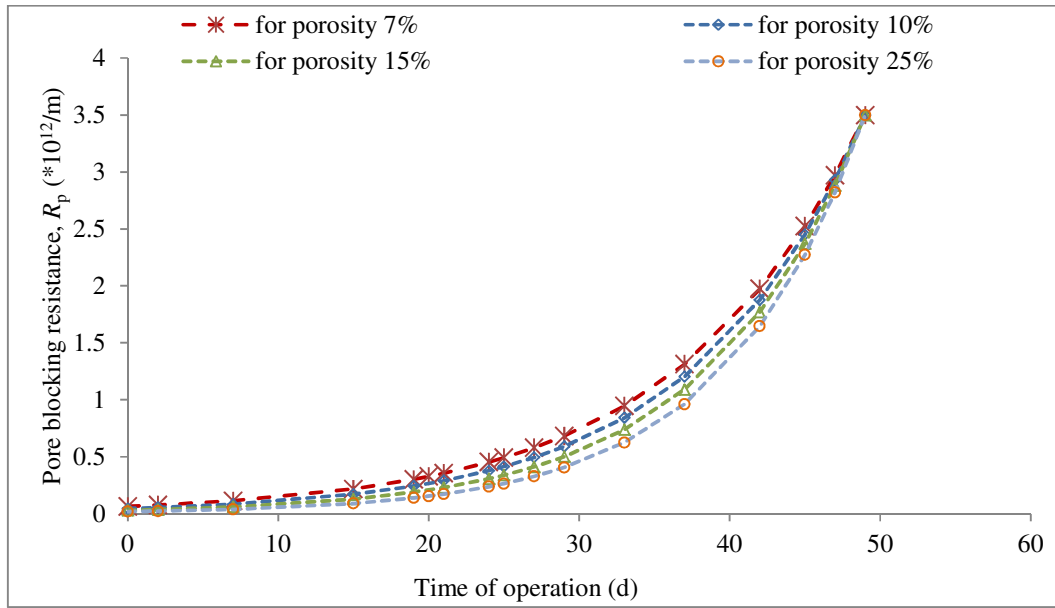


Figure 3

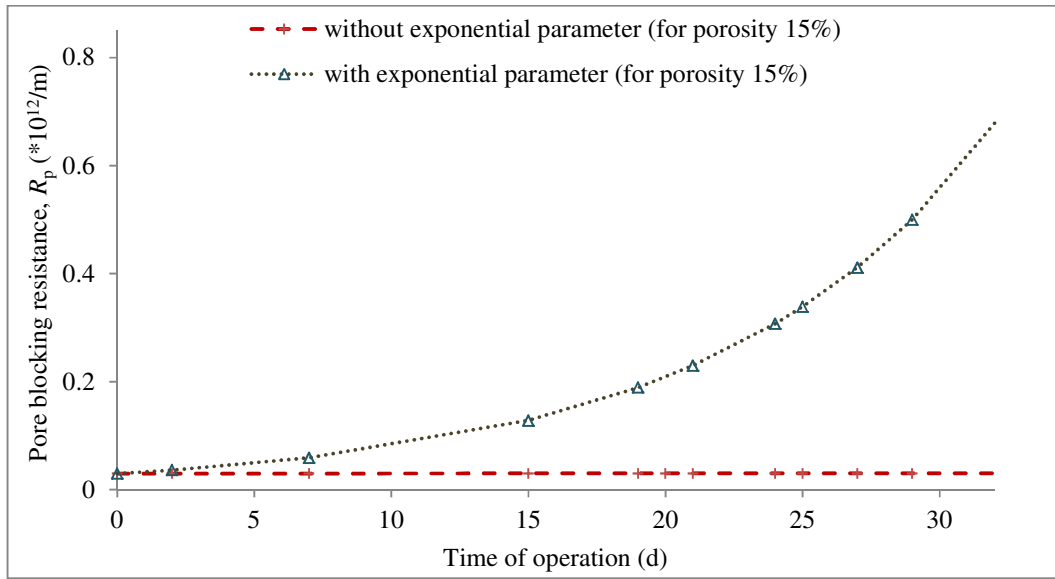


Figure 4

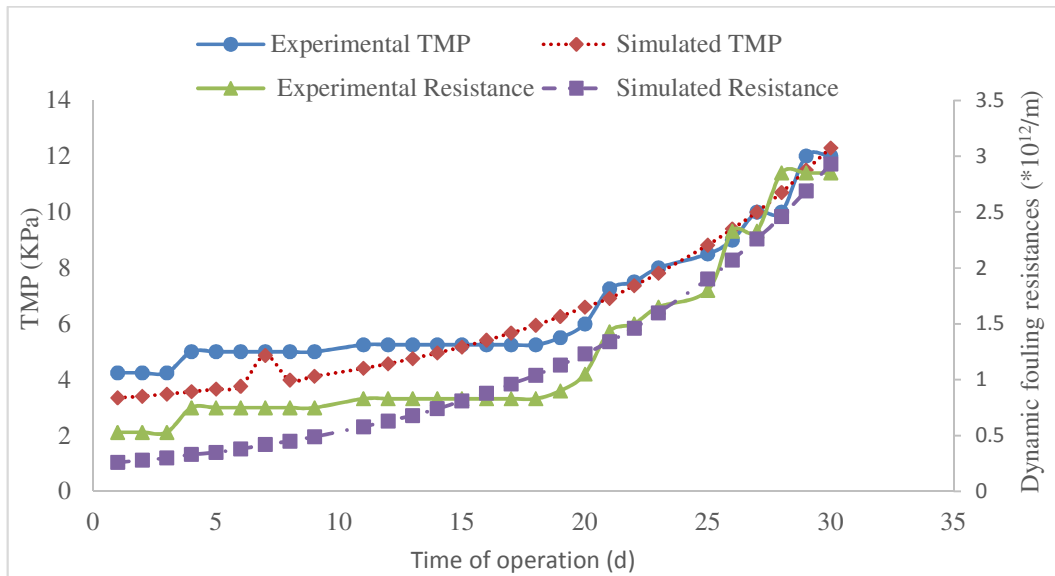


Figure 5

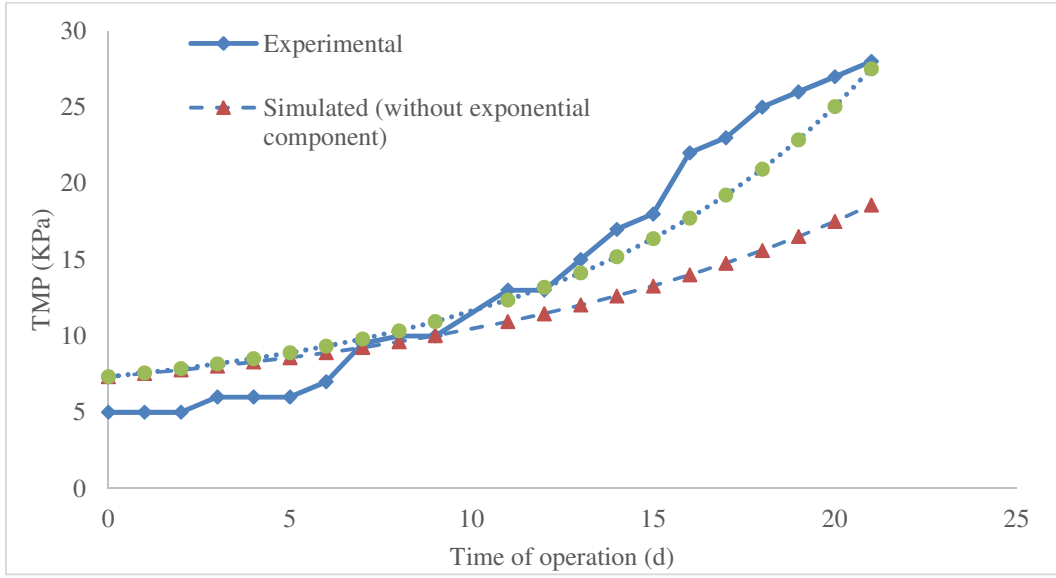


Figure 6